[9]Broadbent, E. G., "Flows with Heat Addition," *Progress in Aerospace Sciences*, Vol. 17, No. 2, 1976, pp. 93–107.

J. A. Martin
Associate Editor

Closed-Form Equations to Evaluate Heat-Pipe-Cooled Leading-Edge Design Feasibility

David E. Glass*
AS&M, Hampton, Virginia 23666

Introduction

WHEN a thermal protection system designer is confronted with a leading-edge design for a hyersonic vehicle, the available options are either passively cooled, heat-pipe-cooled, or actively cooled systems. The upper use limit for passive leading edges may be determined by evaluating the material properties in light of the thermal and mechanical loads. If passive leading edges cannot survive the environmental conditions, heat-pipe-cooled or actively cooled leading edges may be required. Preliminary design studies at NASA Langley Research Center indicate that a refractory-composite/refractory-metal heat-pipe-cooled leading edge can reduce the leading-edge mass by over 50% compared to an actively cooled leading edge, can completely eliminate the need for active cooling, and has the potential to provide fail-safe and redundant features.[1] Though heat pipes are often a viable and lightweight option, the analysis required to determine the feasibility for a particular application can be extensive and can preclude their use. It is therefore beneficial to have a simple set of closed-form equations that can be used to determine if the heat-pipe option is feasible. Having a simple analysis technique available may prevent the unnecessary incorporation of active cooling systems when heat pipes may provide a cheaper and lightweight alternative and may also eliminate the need for a complex, three-dimensional finite element analysis (FEA) to answer the initial question of feasibility.

The purpose of this Note is to present a set of simple, closed-form design equations that can be used to determine a preliminary design of a heat-pipe-cooled leading edge. The design equations presented here are only for thermal design purposes and do not include any stress analysis. Temperatures obtained from the design equations are compared to three-dimensional for both a large and small leading-edge radius. Though some restrictions apply to the use of these equations, they appear to be a useful tool for the preliminary design of heat-pipe-cooled leading edges. Use of these equations will quickly answer questions such as, Is a heat-pipe-cooled leading edge even feasible? What is the heat pipe operating temperature? Are refractory metal or superalloy heat pipes required? Is a refractory-composite structure required? What is the required heat-pipe length? If the preliminary design equations indicate a feasible design, a more detailed analysis should follow.

Design Equations

The design of a heat-pipe-cooled leading edge is very complex because of the numerous variables involved. However, a simple set of closed-form equations is presented here that can be used to determine if a heat-pipe-cooled leading edge is feasible with various material combinations.[2] The equations presented here were developed to model the heat-pipe-cooled leading edge described in Ref. 3, but can be generalized for many other potential designs.

A schematic cross-section diagram of three heat pipes embedded in a structural material is shown in Fig. 1. The heat pipes shown in the figure have a rectangular cross section, but other cross sections could be considered. The leading edge is subjected to aerodynamic heating on the outer surface. At the stagnation line the location of maximum heating, the heating rate, is denoted by q''_{stag}. The thickness of the structure between the outer surface and the heat pipes is denoted by t_s, the outer coating thickness is t_c, and the heat-pipe container wall thickness is t_w. The distance between heat pipes is $2x$, and the width of the heat pipe is w. Contact resistance between the outer surface and the heat pipe is also noted in the figure. The contact resistance on the other surfaces of the heat pipe is of much less concern and is thus neglected. Two paths for the flow of heat from the region of maximum temperature T_{max} to the heat pipe are also shown in Fig. 1 using arrows.

Temperature Difference

The first step is to determine the temperature drop ΔT_{stag} through the structure and heat-pipe container at the stagnation line. This will help dertermine the maximum temperature of the leading edge (T_{max} in Fig. 1), which will occur on the outer surface at the stagnation line, midway between heat pipes. To determine the maximum temperature drop through the structure and heat-pipe container at the stagnation line, the following thermal resistances should be considered: through-the-thickness of the structure (from the outer surface to the heat pipe), in the plane of the structure (from midway between heat pipes to the heat pipe), and the contact resistance. If a coating is used on the outer surface, its thermal resistance (both in-plane and through-the-thickness) should be included. Two conduction paths are shown in Fig. 1 for the heat conducted from midway between heat pipes on the outer surface to the heat pipe. As shown, the heat must be conducted through the coating and structure in the through-the-thickness direction and through the coating and structure in the in-plane direction.

Figure 2 illustrates the approximation of the two-dimensional geometry of Fig. 1 with a thermal resistance network. The thermal resistance is for the heat conduction midway between heat pipes on the outer surface to the heat pipe. The through-the-thickness resistance in the structure is shown in Fig. 2 prior to the in-plane resistances but could be placed after the in-plane resistances with the same result. Other resistance networks could also be used, but care must be exercised because of inconsistent geometric areas. The thermal resistance through the heat-pipe container is neglected

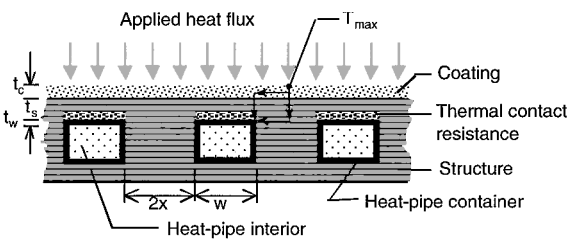

Fig. 1 Schematic of three heat pipes embedded in structure.

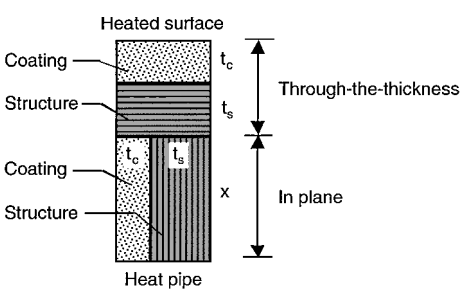

Fig. 2 Schematic drawing of the resistance network for heat to be conducted from midway between heat pipes on the outer surface to a heat pipe.

Received 3 June 1999; revision received 5 August 1999; accepted for publication 28 August 1999.

*Aerospace Engineer; currently TPS and Hot Structures Lead, Mail Stop 396, NASA Langley Research Center, Hampton, VA 23681. Associate Fellow AIAA.

because it is small relative to the other terms and because the heat-transfer area is not consistent with the other terms.

Knowing the stagnation heat flux q''_{stag}, the dimensions, and the thermal conductivities, the temperature drop from a point midway between heat pipes on the outer surface to the heat pipe ΔT_{stag} can be determined from

$$q''_{\text{stag}} = \frac{\Delta T_{\text{stag}}}{\Sigma R} = \Delta T_{\text{stag}} \Bigg/ \left\{ \frac{t_c}{k_c} + \frac{t_s}{k_{s,t}} + \left(\frac{k_{s,p} t_s/(t_s + t_c)}{x} + \frac{k_c t_c/(t_s + t_c)}{x} \right)^{-1} \right\} \tag{1}$$

The stagnation heat flux should be a hot-wall heat flux using the average leading-edge surface temperature. The thermal resistance given in Eq. (1) is for the geometry shown in Fig. 2. The first two resistance terms represent the through-the-thickness series resistance through the coating and structure. The third term represents the in-plane parallel resistance through the coating and structure. The thickness ratios $t_s/(t_s + t_c)$ and $t_c/(t_s + t_c)$ represent the cross-sectional area (assuming a unit depth) for the heat conduction through each layer.

The maximum value of the stagnation heat flux is used, and the transient nature of the heating is not taken into account. Although this is a conservative approach, the thermal response of the leading edge will often be rapid enough that a steady-state approximation at the time of maximum heating will provide relatively accurate temperatures.

Average Surface Temperature

The next step is to determine the average surface temperature based on an assumed heat-pipe length. To determine this temperature, one must know the heat-flux distribution and estimate the chordwise length of the heat pipes on both the upper and lower surface. The heat pipes will normally be oriented perpendicular to the leading edge (chordwise direction) but could be oriented closer to the flow direction for large leading-edge sweep angles. For a swept leading edge orienting the heat pipes perpendicular to the leading edge results in easier fabrication and lower axial heat-pipe acceleration loads. From the heat-flux distribution the integrated heat flux q_{tot} can be obtained for the entire chord length, both upper and lower surfaces, for a spanwise (parallel to the leading edge) unit width. The average external surface temperature (which is relatively uniform because the leading edge is heat-pipe cooled) T_{surf} can then be estimated from

$$q_{\text{tot}} = \varepsilon \sigma A \left(T^4_{\text{surf}} - T^4_{\text{amb}} \right) \tag{2}$$

Thermal radiation to the leading edge from the ambient is included in Eq. (2), but can usually be neglected for most flight profiles. Reducing the upper or lower surface length of the heat pipes, L_u or L_l respectively, will raise the average surface temperature. The area A is based on a unit width (1-in.-wide strip) for the total length of the heat pipe $(L_u + L_l)$. For sharp leading edges on vehicles at small angles of attack, the heat flux drops off in a short distance, usually allowing the radiation equilibrium temperature to drop below the material reuse temperatures in a short distance. However, for very blunt leading edges at high angles of attack, high heat fluxes will extend a significant distance from the stagnation line, resulting in long heat-pipe lengths on both the upper and lower surface.

Heat-Pipe Operating Temperature

The third step is to estimate the internal heat-pipe temperature. The assumption is made that the heat pipe is at uniform temperature and thus the heat radiated from the surface is also uniform. First, the heat flux out of the heat pipes is calculated assuming that the heat flux radiated from the leading-edge outer surface must first be conducted through the heat-pipe width w. The distance between heat pipes is $2x$, and, thus, for every spanwise unit width of leading edge, the heat flux must be conducted through a heat pipe of width w, but is radiated from the outer surface over a width of $w + 2x$. Therefore, for each 1-in.-unit width of leading edge, the heat is conducted to the outer surface through a width of (1 in.) $w/(w + 2x)$. The average heat flux conducted through the wall of the heat-pipe container is then

$$q''_{\text{avg}} = q_{\text{tot}} / \{(L_u + L_l)(1\text{ in.})[w/(w + 2x)]\} \tag{3}$$

Knowing the average heat flux, the temperature drop through the structure and heat-pipe container, $\Delta T_{s,\text{hp}}$ can be obtained from

$$q''_{\text{avg}} = \Delta T_{s,\text{hp}} / (t_{s,t}/k_{s,t} + t_w/k_w + t_c/k_c + 1/h_{\text{cr}}) \tag{4}$$

Note that in Eq. (4) there is no in-plane thermal resistance. Contact resistance h_{cr} between the heat pipe and structure, if known, can be included in Eq. (4). However, it is well known that thermal contact resistance is extremely dependent on geometry, pressure, material, and temperature, making modeling of this parameter difficult to incorporate. The heat-pipe operating temperature is then obtained from

$$T_{\text{hp}} = T_{\text{surf}} - \Delta T_{s,\text{hp}} \tag{5}$$

Maximum Surface Temperature

The final value to obtain is the maximum leading-edge temperature, which will occur midway between heat pipes at the stagnation line. This temperature is obtained from

$$T_{\text{max}} = T_{\text{hp}} + \Delta T_{\text{stag}} \tag{6}$$

Discussion

The important parameters for a heat-pipe-cooled leading edge have now been obtained for an assumed geometry and material system: the maximum surface temperature T_{max} and the heat-pipe operating temperature T_{hp}. A comparison of the calculated maximum surface temperature with the reuse temperature of the coating and structural materials will determine if they are feasible for the given application. Several iterations may be required to obtain a design with acceptable temperatures using the corresponding material properties and geometry.

Because a heat pipe redistributes thermal energy instead of removing it as in active cooling, the total energy balance is extremely important. For this reason sharp leading edges are better suited for heat-pipe cooling than blunt leading edges. A blunt leading edge will have a lower stagnation heat flux than a sharp leading edge under the same flow conditions; however, it will likely have a higher integrated heat load. As a result, the surface area required to radiate the energy away may be larger, i.e., longer heat pipes are required.

Low angles of attack are more conducive to heat-pipe cooling than high angles of attack. A high angle of attack will heat a larger portion of the lower surface, making it less useful for radiating away heat transferred from the stagnation region. The heat must thus be moved to the upper surface, which experiences very little heating. The required heat-pipe lengths are therefore much longer than for a corresponding low-angle-of-attack leading edge.

The approximation presented here conservatively estimates the maximum temperatures by assuming no transfer of heat chordwise at the stagnation line. However, because of the sharp reduction in heat flux at the stagnation line, three dimensions should be considered for a complete detailed analysis. For sharp leading edges heat will be transferred away from the stagnation line in the chordwise direction parallel to the heat pipes, thus reducing the leading-edge temperatures and resulting in a conservative approximation. For blunt leading edges the chordwise heat-flux reduction is much less, and the three-dimensional effect is correspondingly less significant.

A second conservative feature of this technique is the use of a constant applied heat flux on the outer surface with only radiation losses. For actual aerodynamic heating the reduction in the applied heat flux with rising surface temperature is much greater if convection to a hot surface is considered rather than assuming a constant heat flux with radiation losses alone. This effect is most pronounced as the heat-pipe spacing increases. For very small heat-pipe spacing the surface temperature, and thus heat flux, is relatively uniform. For large heat-pipe spacing the maximum temperature between heat pipes is much greater than directly over a heat pipe. If surface-temperature-dependent convective aerodynamic heating is considered instead of a constant applied heat flux, the aerodynamic

Table 1 Comparison of design and FEA temperatures

Case	$T_{hp,design}$, °F	$T_{hp,FEA}$, °F	Difference, °F	$T_{max,design}$, °F	$T_{max,FEA}$, °F	Difference, °F
Blunt leading edge, q_{stag} = 83 Btu/ft^2-s and r = 9 in.						
Test case 1 (q_{tot} = 11.6 Btu/s, t_s = 0.04 in., x = 0.7 in., L_u = 24 in.)[a]	2,587	2,556	31	3,394	3,243	151
Test case 2 (q_{tot} = 12.09 Btu/s, t_s = 0.04 in., x = 0.05 in., L_u = 36 in.)[a]	2,530	2,420	110	2,670	2,505	165
Test case 3 (q_{tot} = 11.6 Btu/s, t_s = 0.25 in., x = 0.7 in., L_u = 24 in.)[a]	1,933	2,525	592	3,145	3,074	71
Test case 4 (q_{tot} = 11.6 Btu/s, t_s = 0.25 in., x = 0.05 in., L_u = 24 in.)[a]	2,455	2,537	82	3,003	2,821	182
Sharp leading edge, q_{stag} = 750 Btu/ft^2-s and r = 0.5 in.						
Test case 5 (q_{tot} = 19.142 Btu/s, t_s = 0.04 in., x = 0.05 in., L_u = L_l = 24 in.)[a]	2,968	3,036	68	4,230	4,077	153
Test case 6 (q_{tot} = 22.906 Btu/s, t_s = 0.04 in., x = 0.05 in., L_u = L_l = 36 in.)[a]	2,791	2,851	60	3,962	3,926	36
Test case 7 (q_{tot} = 19.142 Btu/s, t_s = 0.04 in., x = 0.7 in., L_u = L_l = 24 in.)[a]	2,826	2,985	159	10,121	6,064	4,057

[a]All other variables are the same as in Table 2.

heating applied to the surface will decrease significantly with the rise in surface temperature. The convection boundary condition thus results in a damping of the temperature rise.

The equations presented here are used to determine the heat-pipe temperature and the maximum surface temperature. An average surface temperature is first used to determine the heat-pipe temperature, and then a temperature at the stagnation line is used to obtain the maximum leading-edge temperature from the heat-pipe temperature. In reality, the surface temperature will not be uniform due to the thermal resistances of the composite structure within which it is embedded. The surface temperature will be higher than the heat-pipe temperature in the evaporator and lower than the heat-pipe temperature in the condenser. An alternate set of equations was derived utilizing different evaporator and condenser surface temperatures. The location and temperature of the evaporator/condenser boundary was determined by iteration. Though the surface temperatures were thought to be more accurate because they took into account that the evaporator and condenser surface temperatures were different, the heat-pipe temperatures indicated no increase in accuracy. The temperature from the heat pipe to the maximum surface temperature was exactly the same because it is based only on resistances in that region. With no increased accuracy in the two key temperatures for design feasibility (heat-pipe temperature and maximum surface temperature) by using the more rigorous iterative approach, the single surface temperature set of equations has been presented here.

Comparison of Design and FEA Results

A comparison of the heat-pipe temperature and maximum surface temperature are summarized in Table 1 for the design equations and a full three-dimensional FEA for a blunt leading edge such as on the Space Shuttle Orbiter. The FEA results are intended to provide representative temperatures for each condition. The accuracy of the FEA was previously verified, and a detailed discussion of the FEA is presented in Ref. 1. Although the FEA has a nonlinear property capability, the constant properties in Table 2 were used in the FEA to provide a true comparison with the design equations. In each case the variables that are different from those in Table 2 are listed in Table 1 (all other variables are the same as in Table 2).

Test cases 1–4 are for a blunt leading edge (r = 9 in.) with a relatively low heat flux and a large angle of attack. Test case 2 has a much smaller half heat-pipe spacing than in test case 1 (0.05 in. vs 0.7 in.) and a longer upper surface heat-pipe length. The longer upper surface heat pipe results in a slightly larger integrated heat load. In test case 3 the thickness of the structure beneath the coating is increased to 0.25 in., and the half spacing between heat pipes is 0.7 in. Both of these dimensions are relatively large and result in a heat-pipe temperature that is quite low. The combination of a thick structure above the heat pipe and a relatively large distance between heat pipes results in a large thermal resistance and thus a large temperature difference between the outer surface and the heat pipe. The larger dimensions also result in the approximation being less accurate. In test case 4 the structural thickness is still large, but the heat pipes are spaced much closer; the heat-pipe temperature from the design equations is much closer to that from the FEA.

Table 2 Baseline variables for comparison of results

Variable	Value
t_s	0.04 in.
t_w	0.01 in.
t_c	0.01 in.
x	0.7 in.
L_u	24 in.
L_l	18 in.
r	9 in.
$k_{s,t}$	12.8 Btu/h-ft-°F
$k_{s,p}$	24.408 Btu/h-ft-°F
k_w	39.485 Btu/h-ft-°F
k_c	23.587 Btu/h-ft-°F
ε	0.8

Three cases are presented for a sharp leading edge (r = 0.5 in.) with a higher heat (q_{stag} = 750 Btu/ft^2-s) in Table 1. The angle of attack for test cases 5–7 is near zero. The design results compare well with the FEA except for large heat-pipe spacing (test case 7), where the maximum temperatures obtained by the two methods are very different because as the heat-pipe spacing increases the problem becomes more three-dimensional, and the design equations become less accurate. However, both the design equations and the FEA indicate that the design with large heat-pipe spacing is not feasible. The design equations presented here can be used relatively accurately to obtain a preliminary design assuming closely spaced heat pipes. Once it is determined that heat pipes are feasible with closely spaced heat pipes, a more detailed analysis should be performed to determine optimum heat-pipe spacing.

Conclusion

A set of closed-form equations has been presented to obtain a preliminary design of a heat-pipe-cooled leading edge for hypersonic

vehicles. The results from the design equations were compared with results from a three-dimensional FEA for both a large and a small leading-edge radius. The results compared quite well for most cases and indicate that the equations can be used for a quick assessment of a preliminary heat-pipe-cooled leading-edge design. If a feasible design is indicated, a more detailed analysis should follow.

Acknowledgment

The author would like to thank the Thermal Structures Branch at NASA Langley Research Center for funding this work under Contract NAS1-96014.

References

[1]Glass, D. E., and Camarda, C. J., "Preliminary Thermal/Structural Analysis of a Carbon-Carbon/Refractory-Metal Heat-Pipe-Cooled Wing Leading Edge," *Thermal Structures and Materials for High Speed Flight*, edited by E. A. Thornton, Vol. 140, Progress in Astronautics and Aeronautics, AIAA, Washington, DC, 1992, pp. 301–322.

[2]Glass, D. E., "Closed Form Equations for the Preliminary Design of a Heat-Pipe-Cooled Leading Edge," NASA CR-1998-208962, Dec. 1998.

[3]Glass, D. E., Camarda, C. J., Merrigan, M. A., and Sena, J. T., "Fabrication and Testing of Mo-Re Heat Pipes Embedded in Carbon/Carbon," *Journal of Spacecraft and Rockets*, Vol. 36, No. 1, 1999, pp. 79–86.

M. Torres
Associate Editor

Effects of Arcing on Insulator Surface Potential in Plasma: Image Observation

Mengu Cho,* Naoki Miyata,† and Masayuki Hikita‡
Kyushu Institute of Technology,
Kitakyushu 804-8550, Japan

Introduction

THE use of high power in future space missions, especially in low Earth orbit (LEO), calls for high-voltage power generation and transmission, typically higher than 100 V. When solar arrays generate electrical power at a high voltage, most of the voltage becomes negative with respect to the plasma due to the low mobility of ions.[1] Arcing is known to occur at the negative part of the solar array. The arcing causes various undesired side effects, such as electromagnetic interference and surface deterioration and sometimes leads to the permanent loss of the spacecraft power, such as the case of the Tempo-2 satellite.[2] Preventing arcing is an important technical task to realize a large space platform in LEO that uses high power of the order of 100 kW or more.

A conventional design of solar arrays has a series of solar cells connected by exposed interconnectors with coverglasses placed on top of the cells. The triple junction is formed by the interconnector (electrical conductor), the coverglass (electrical insulator), and the surrounding plasma. Studies on high-voltage solar arrays (see Ferguson et al.[2] and references therein) revealed that arcing occurs at the triple junction once a strong electric field is applied by the charging of the dielectric material. Thieman et al.[3] observed optical flashes along the edge of the coverglass. Vaughn et al.[4] showed that an arc produced a dense plasma that neutralized the positive surface on the nearby dielectric surface.

Cho et al.[5] proposed that the arc rate is given as the inverse of the charging time. The coverglass surface is charged by positive ions that are attracted by the negative potential of the solar cells. At steady state, the surface potential is nearly equal to the space plasma potential. Then, the insulator surface near the triple junction is charged further by secondary electron emission that is released by the impact of electrons emitted from the interconnector surface via field emission. Once an arc occurs, the arc plasma neutralizes the positive charge near the arc spot, and the charging process restarts.

The purpose of this paper is to present the results of direct observation of the charging and discharging process near the arc spot. We have developed an experimental system, which can measure the in situ two-dimensional surface potential distribution over the dielectric material placed in a plasma environment. The system employs a nonlinear optical crystal, $B_{i12}S_iO_{20}$ (BSO), which exhibits the Pockels effect. Miller[6] measured the surface potential by sweeping an electrostatic probe, which disturbed the plasma environment near the test sample and often caused arcing as the probe moved over the exposed conductor. The observation system used in this paper is an optical method and can measure the charge distribution without disturbing the environment near the test sample.

Experiment

Figure 1 shows a schematic of the experimental system. The pressure in the vacuum chamber (1 m diameter and 1.2 m length) is 8×10^{-2} Pa when the diffusive argon plasma source is operated. The plasma density is 10^{11} m^{-3}, and the electron temperature is 1 eV. The plasma potential with respect to the grounded chamber wall is approximately +10 V. The test sample consists of an indium tin oxide (ITO) electrode (4 × 4 cm), BSO crystal (1 × 1 cm and 1 mm thickness), and polyimide film (25 μm thickness). The test sample is placed on acrylic plate and biased to −1 kV. The BSO

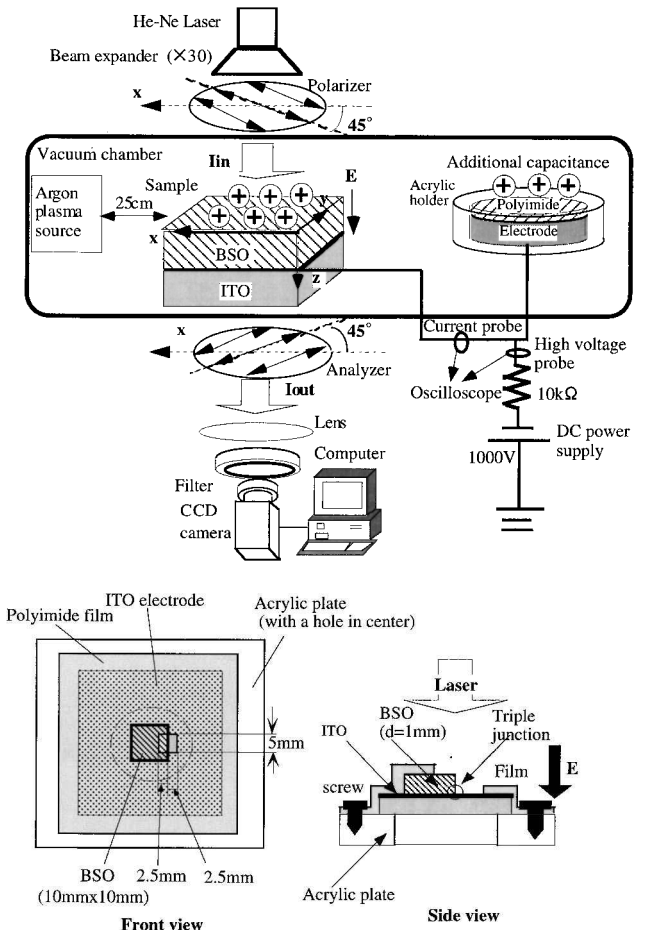

Fig. 1 Schematic of experiment setup.

Received 9 July 1999; revision received 5 October 1999; accepted for publication 9 October 1999.

*Associate Professor, Department of Electrical Engineering. Member AIAA.

†Graduate Student, Department of Electrical Engineering; currently Engineer, Power Division, Shikoku Electric Power Co., Inc., Matsuyama 790-0951, Japan.

‡Professor, Department of Electrical Engineering.